AUT Journal of Electrical Engineering

AUT J. Elec. Eng., 58(1) (2026) 167-188
DOI: 10.22060/eej.2025.24451.5707

Electric–Thermal Sector Coupling with Hybrid Renewables and Storage for Sustainable Rural Energy Systems

Elham Sadeghi, Mostafa Gholami*

Department of Electrical Engineering, University of Science and Technology of Mazandaran, Behshahr, Iran.

ABSTRACT: With the increasing importance of electrical energy in daily life, power outages pose serious challenges. Globally, efforts are made to ensure access to electricity for all, especially in rural areas that are often remote. Similar difficulties exist in meeting thermal loads, often addressed through natural gas networks—solutions that are costly and logistically complex. This paper investigates the strategic integration of hybrid renewable energy systems and storage technologies to enable sector coupling, thereby allowing coordinated management of both electrical and thermal loads in rural regions. By utilizing sector coupling, the proposed approach improves energy efficiency, decreases fossil fuel dependence, and supports sustainable development. Thermal load control is employed as an interface between electrical sources and thermal demand, increasing the share of renewables. The study begins by analyzing various off-grid hybrid energy system models and then evaluates the impact of factors such as natural gas prices, system reliability, costs, and emissions. Additionally, a sensitivity analysis on declining battery investment costs is conducted to assess their influence on system economics and renewable penetration. A comparative benchmark using a natural gas generator with heat recovery is also examined to highlight the techno-economic advantages of the proposed system configuration. Results show that deploying off-grid hybrid systems and accepting a degree of reduced reliability can notably increase the contribution of renewables in supplying simultaneous electric and thermal loads. This shift leads to significant reductions in pollutant emissions and fosters sustainable rural development—achieved without the prohibitive expenses tied to expanding electricity and gas infrastructure.

Review History:

Received: Aug. 02, 2025
Revised: Oct. 18, 2025
Accepted: Nov. 14, 2025
Available Online: Jan. 10, 2026

Keywords:

Hybrid Systems
Wind Turbines
Thermal Load Control
Photovoltaic
Renewable Energy
Sustainability

1- Introduction

Nowadays, electrical energy is an inseparable part of human life. However, the electrical energy of approximately 2.4 billion people is limited or unreliable [1]. Electricity with low reliability is mostly observed in the rural areas of developing countries. While reliable electric energy can have a significant impact on their economic growth and welfare, and reduce the trend of their migration to cities [2], The global challenge of energy access remains significant. The International Energy Agency (IEA) reports that between 2022 and 2023, an additional 507 GW of renewable electricity capacity was introduced, marking a 50% increase worldwide. Nevertheless, fossil fuels continued to account for 60% of the total electricity production globally in 2023, highlighting the urgent need for a transition to renewable energy sources (RESs) [3].

In contrast, many villages are located at great distances from cities, and given their low population, electrification through the grid with high investment cost is not justifiable [4]. The high initial investment, low load factors, and inadequate voltage regulation create obstacles in providing grid electricity to these villages [5]. Besides, the traditional approach to supplying new electricity connections, primarily relying on conventional sources such as fossil fuels, is not a sustainable solution. The increasing environmental costs and fuel prices render the extension of the grid both costly and less appealing [6].

The renewable energy (RE) sector has achieved remarkable cost competitiveness, with solar electricity prices plummeting by 85% and wind power costs dropping by 56% (onshore) and 48% (offshore) between 2010 and 2020 [7]. Wind energy, in particular, offers several advantages as a reliable and clean source of power. Wind turbines utilize an abundant natural resource available day and night, reduce environmental pollution through zero-emission operation, and contribute to lowering electricity generation costs compared with fossil fuels [8].

With the growth of RE technologies, it is now possible to supply the necessary electrical power to rural areas independently, without the need to expand the grid [9]. The expansion of solar and wind energy utilization, along with energy storage systems, has created the possibility of eliminating the need to expand the grid in inaccessible areas.

The growing effects of global warming, alongside the

*Corresponding author's email: m.gholami@mazust.ac.ir

limited availability of conventional energy sources, have underscored the urgent need for the implementation of sustainable measures worldwide [10]. The use of traditional power sources, including fossil fuels, increases greenhouse gas emissions and environmental pollution. Thus, renewable energy sources have attracted considerable attention over the past decade [11]. Research indicates that utilizing RESs, enhancing energy efficiency, and electrifying end-uses have resulted in a 94% reduction in greenhouse gas emissions [12]. Therefore, providing energy for rural areas using RESs can not only meet their energy needs but also help preserve the environment and reduce pollution. Moreover, the instability of oil and natural gas prices poses a significant challenge to energy planning and sustainability [13], especially in remote or off-grid regions where the extension of conventional infrastructure is economically unfeasible.

This RE transition becomes even more impactful when applied through sector coupling. This approach involves the integrated optimization of energy generation and consumption across multiple sectors. Particularly in rural areas, where energy systems often operate in isolation, sector coupling enables more efficient energy use. One effective approach to achieving sector coupling is the substitution of electrical energy for fossil fuels, particularly natural gas, to meet heating demands in rural areas. By integrating RESs with thermal load controllers (TLCs), this strategy not only reduces emissions but also enhances the synergy between electrical and thermal energy systems, paving the way for sustainable development [14].

Many rural areas in Iran with more than 20 households have gained access to the electrical grid and gas supply system in recent decades. This form of electricity and gas distribution is unjustifiable for many villages and is only extended due to social responsibility and the observance of citizen rights.

Iran enjoys an average of 300 sunny days per year, along with significant wind energy potential in various regions, making it an ideal candidate for RE adoption in rural areas [15]. Fig. 1 highlights Iran's significant solar energy potential. Table 1 provides a detailed comparison of Global Horizontal Irradiation (GHI) levels between Iran and Germany. As a leading country in solar energy utilization, by 2024, Germany had installed over 90 GW of solar energy capacity [16]. The average GHI in Iran (5.52) is 1.85 times higher than the

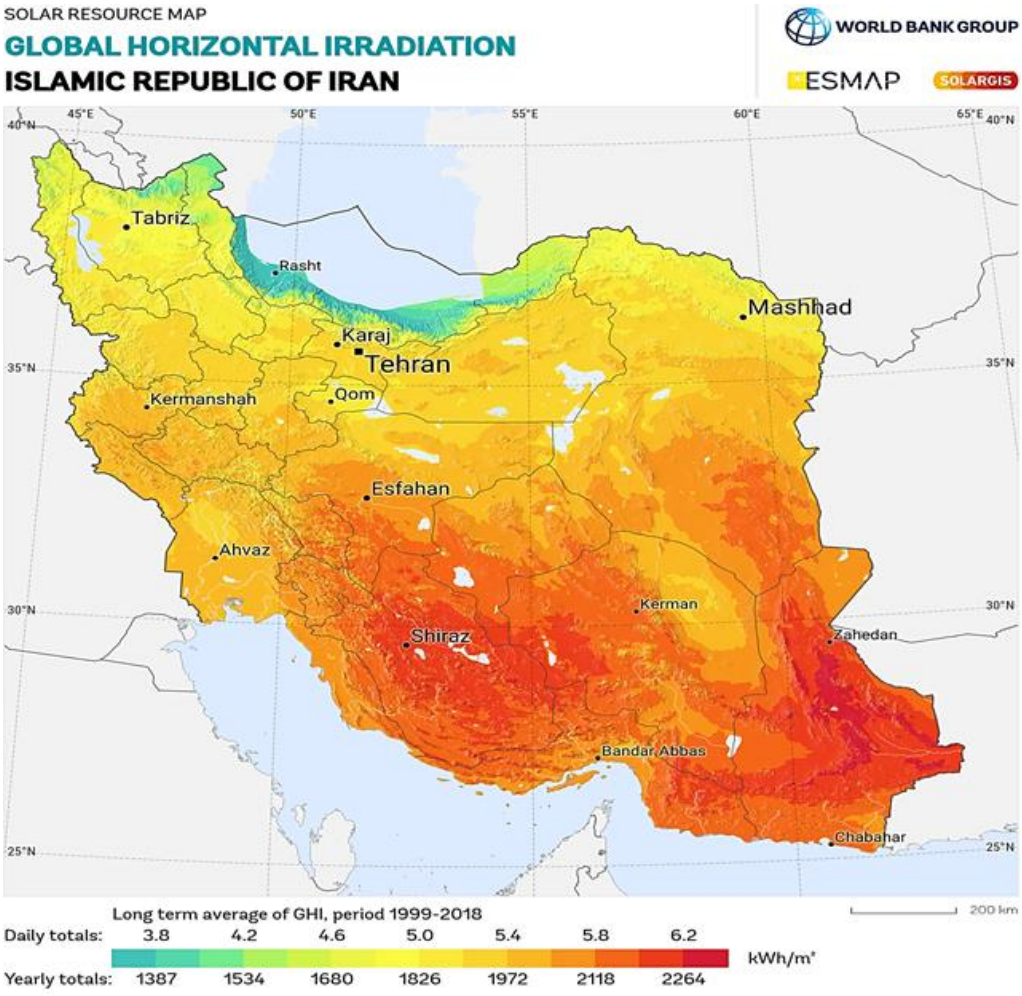

Fig. 1. The opportunities for solar power in Iran [17].

Table 1. Evaluating the Global Horizontal Irradiation (GHI) levels in Iran versus Germany [17].

Statistics of GHI	Iran	Germany
Average (kWh/m^2)	5.52	2.98
Maximum (kWh/m^2)	6.23	3.34
Percentile 75 (kWh/m^2)	5.86	3.09
Percentile 50 (Median) (kWh/m^2)	5.56	2.95
Percentile 25 (kWh/m^2)	5.31	2.86
Minimum(kWh/m^2)	3.67	2.75

average GHI in Germany (2.98). Therefore, Iran has a very suitable solar energy potential that, with proper planning, can be utilized to meet the energy needs of rural areas. Increasing the utilization of this potential in Iran could lead to a reduction in pollutant emissions and grid extension costs.

Although integrating RE into the electricity grid presents significant advantages for the environment and sustainability, it still faces considerable challenges. The main reason for this lies in the unpredictable nature of RESs. This uncertainty plays a significant role in the shift towards a hybrid energy model. By combining various energy sources, the reliability of the system improves. Such integration helps to reduce the effects of fluctuations caused by weather on RES's output power [18]. Consequently, when energy generation from one source decreases, other sources can compensate for the shortfall [10]. Additionally, energy production from wind and photovoltaic sources tends to balance out over different seasons or even on daily cycles due to varying weather and climate conditions [19]. Besides, the advancement in battery-based storage systems is able to address the problems caused by the uncertainty of these sources and establish a balance between energy production and consumption [20, 21].

Finding an optimal design for a hybrid renewable energy system (HRES) requires consideration of various factors such as local RE resources, load profile, expected reliability, inflation rate, carbon emissions taxes, and capital and maintenance costs [22]. The impact of different load types (residential, commercial, school, Industrial, and hospital) on the design of HRES is evaluated in [23]. These considerations are crucial for designing systems that are both economically viable and environmentally sustainable [24]. Furthermore, energy management strategies play a pivotal role in hybrid energy systems by coordinating power flows among diverse energy sources with distinct dynamic behaviors [25]. In such systems, the integration of AC and DC energy sources and loads requires intelligent supervisory controllers to efficiently manage the power flow and maintain system reliability under varying operational modes [26].

Various articles have examined the use of HRES with different combinations, such as solar, wind, biomass, diesel generators, and batteries, alongside access to the grid [10, 22, 27, 28]. In [10], it is suggested that a portion of the electrical demand of an on-grid refinery unit be supplied by HRES. In [22], a HRES that includes solar, wind, and biomass is proposed to fulfill the energy needs of a rural area connected to the grid. The impact of economic variables such as the nominal discount rate and expected inflation rate on the optimal architecture and costs of the HRES is investigated in [22]. In [27], The use of a HRES to meet the electrical requirements of a grid-connected microgrid with controllable loads is suggested. The proposed HRES in [27] includes RESs, storage, and a diesel generator to ensure the provision of critical demands during grid outages by shedding controllable loads. In [28], horizontal and vertical axis wind turbines are compared within a HRES that includes solar and wind resources alongside the grid to meet household loads.

Furthermore, some studies have focused on off-grid HRES. In [29], a HRES consisting of PV/biomass/diesel generator/battery energy storage is employed to meet the electrical demand of an off-grid rural area in Bangladesh. Besides, Reference [29] has explored various electricity pricing structures to identify a feasible and effective payback period for this initiative. In [30], the study utilizes HRES to meet the electrical energy demand of an area at different scales within a city using renewable resources. Reference [31] focuses on optimizing the capacity of a biomass-based PV system intended to provide electrical energy for agricultural wells in Bardsir, Kerman, Iran. By combining PV and biomass systems, the study aims to develop a reliable and economically viable HRES, considering the complementary properties of these RESs. In [32], an optimum design of the HRES consisting of PV/wind/biogas is presented for rural electrification. The authors analysed the techno-economic performance of this system while considering various load patterns and calculating their variations through short-term load forecasting techniques. Agri-PV systems, which combine agricultural production with photovoltaic energy generation, offer a promising solution to address both energy and food security challenges, particularly in regions where land availability is limited [33].

In all the aforementioned studies, the focus has primarily been on electrical energy consumption. In addition to

Table 2. Evaluating a comparative summary of related works and identifying research gaps.

Reference	System Configuration	Considered Sectors	Optimization / Simulation tool	Main Objectives	Limitations
[29]	PV / Biomass / Diesel / Battery	Electrical	Homer	Techno-economic feasibility of off-grid hybrid mini-grid for rural electrification in Bangladesh	Focused only on electricity; no integration of thermal energy or sector coupling
[32]	PV / Biomass	Electrical	harmony search (an efficient heuristic optimization technique)	optimizing the size of a biomass-based PV power plant to supply the electrical power of agricultural wells located in Iran	Focuses only on electrical energy; no consideration of heating or sector coupling
[34]	combined-heat-and-power (CHP) and power-to-heat (PtH) systems	Electrical & Thermal	Analytical and review-based (no simulation tool used)	Review of CHP and PtH systems for sector coupling and frequency control in microgrids.	Theoretical review; no practical case study or techno-economic optimization
This Study	PV / Wind / Battery / TLC	Electrical & Thermal	HOMER	Techno-economic design and optimization for rural Iran	-

electrical energy requirements, remote rural areas also rely on gas for heating, cooking, and other applications. Therefore, it is crucial to investigate the thermal and electrical sector coupling [34] and simultaneous use of RE for both sectors in a technical-economic assessment. This gap in research is the primary concern addressed in this study, as transitioning heating systems to electric options could significantly reduce emissions and contribute to sustainable development.

Table 2 summarizes the key characteristics and research gaps of the most relevant studies, particularly Refs. [27], [30], and [32], in comparison with the present work. As can be observed, most previous studies have focused solely on the electrical domain, neglecting the potential benefits of integrating the thermal sector. To bridge this gap, the present study proposes an electrical–thermal HRES tailored for rural areas by integrating a TLC to manage heating demand alongside electrical energy, thereby enhancing overall system energy efficiency. Furthermore, this work implements a practical optimization of electrical–thermal coupling within a rural HRES using HOMER software, contributing to a more comprehensive understanding of energy management in rural electrification scenarios.

As summarized in Table 2, previous studies have typically addressed reliability, stability, and economic optimization in isolation, focusing either on electrical or thermal domains or examining frequency control in the context of grid-connected microgrids. In contrast, the present study develops a unified electrical–thermal HRES model for rural off-grid applications that simultaneously captures technical and economic interactions between the two sectors. While dynamic frequency regulation is a central concern for interconnected (grid-connected) microgrids with low inertia, our off-grid study concentrates on steady-state techno-economic optimization and coordinated energy management (including thermal load control), rather than dynamic frequency control. This integrated perspective enables evaluation of reliability–cost trade-offs under realistic off-grid operating conditions and supports practical optimization of electrical–thermal coupling.

The impact of reliability on the costs of off-grid HRES is another aspect that is overlooked in the literature. To achieve a highly reliable off-grid system, significant capital investment is required for energy generation resources and storage facilities. These costs arise from the uncertainty in RE production. However, considering a lower level of reliability for the system results in cost reduction. Therefore, it is necessary to assess the effect of system reliability on costs.

In this paper, a HRES comprising solar energy, wind energy, and battery-based storage is designed and optimized for a village in Yazd Province in Iran. The primary aim of this paper is to conduct a techno-economic assessment of HRESs for coupling two sectors of power and heat to small and remote rural areas on an off-grid basis. Moreover, the impact of the expected reliability level and natural gas fuel price on the system's architecture and costs is examined.

In addition, considering the rapid development of battery technologies and their significant contribution to system investment costs, a sensitivity analysis is conducted to evaluate the effect of declining battery capital costs on the techno-economic performance of the proposed system.

The main innovations of this paper are summarized as follows:

- Development of a coupled electrical–thermal HRES configuration specifically tailored for rural off-grid applications.

- Integration of a TLC to manage heating demand alongside electrical energy, enhancing overall system efficiency and operational flexibility.
- Unified techno-economic optimization of electrical–thermal coupling using HOMER software.
- Evaluation of the influence of reliability level, natural gas fuel price, and battery investment cost on the optimal design and cost of the off-grid HRES.

The remainder of the paper is structured as follows: In Section 2, the system modelling is presented. Section 3 describes the proposed method. In Section 4, the implementation results are provided. Finally, conclusion is presented in section 5.

2- System Modelling

The proposed system layout focuses on sector coupling, integrating thermal and electrical load management by utilizing RESs like solar panels, wind turbines, battery storage systems, and TLCs. This approach ensures the simultaneous and efficient supply of both electrical and thermal energy, optimizing resource utilization and reducing environmental impact. This equipment modelling is introduced in detail in this section.

2- 1- Solar Panels

Solar cells are the basic components in PV power generation. They convert the energy of the sunlight directly into electricity [35]. The output efficiency of solar panels is influenced by several factors, notably the level of irradiation, temperature, and various losses that diminish production capacity [22]. The energy losses occurring in solar panels can be attributed to wiring inefficiencies, deterioration of the panels, and accumulations of dust, snow, and shading [29]. The electrical output of a photovoltaic configuration follows the Equation (1) [22, 36].

$$P_{PV} = Y_{PV} f_{PV} \left(\frac{G_T}{G_{T,STC}} \right) \left[1 + \alpha_P \left(T_C - T_{C,STC} \right) \right] \quad (1)$$

Wherein Y_{PV} represents the rated power of the photovoltaic array in kilowatts; f_{PV} stands for the derating factor coefficient in percentage; G_T and $G_{T,STC}$ correspond to the instantaneous irradiance (kW/m^2) and the irradiance measured under standard test conditions (1 kW/m^2) on the solar panel's surface, respectively. α_P represents the temperature coefficient illustrating the adverse effect of increased surface temperature on the PV array's output power expressed in %/°C; T_C indicates the surface temperature of the panel in °C, while $T_{C,STC}$ represents the surface temperature under standard testing conditions, generally accepted as 25°C [22, 36]. The calculation for *Tc* is given by Equation (2).

$$T_C = T_\alpha + G_T \cdot \left(\frac{NOCT - 20}{800} \right) \quad (2)$$

Where, T_α and *NOCT* are the ambient temperature (°C) and the nominal operating cell temperature (°C), respectively.

Since photovoltaic arrays produce direct current (DC), the efficiency of the DC-AC inverter (η_{inv}) plays a crucial role in determining the power delivered to electrical loads $(P_{inv,out})$, with its impact represented in Equation (3) [22].

$$P_{inv,out} = \eta_{inv} . P_{PV} \quad (3)$$

2- 2- Wind Turbines

A minimum wind velocity, identified as $v_{Cut\text{-}in}$, is necessary for wind turbines to start generating power. Once the turbine attains its rated wind speed (v_{Rated}), its output energy matches the turbine's specified rated power (P_{Rated}). At elevated wind speeds, the turbine, the turbine produces a constant rated power output. To ensure safe operation at elevated wind speeds, the turbine will cease operation, with this maximum threshold defined as $v_{Cut\text{-}out}$ [37, 38]. Notably, the power production of the turbine is governed by the wind speed at hub height. Thus, The power generated by the wind turbine at a given wind speed v ($P_w(v)$) can be formulated in accordance with Equation (4) [39].

$$P_w(v) = \begin{cases} \dfrac{P_{Rated}\left(v - v_{Cut-in}\right)}{v_{Rated} - v_{Cut-in}}, & \left(v_{Cut-in} < v < v_{Rated}\right) \\ P_{Rated}, & \left(v_{Rated} < v < v_{Cut-out}\right) \\ 0, & \left(v < v_{Cut-in} \ \ or \ \ v > v_{Cut-out}\right) \end{cases} \quad (4)$$

As the output power of wind turbines relies on the wind speed at the hub height, and this data is often measured at the height of the anemometer by meteorological services, it becomes necessary to calculate the wind speed specifically at the turbine hub. This is accomplished using Equation (5) [39].

$$v_h = v_{h_0} \times \left(\frac{h}{h_0} \right)^\alpha \quad (5)$$

In this context, v_h represents the wind speed at height h, v_{h0} denotes the wind speed at a benchmark height h_0, and α is a constant factor influenced by numerous variables, including height, time of day, season, geographical characteristics, wind velocity, and temperature [40].

2- 3- Battery Energy Storage

Considering the variations in irradiance conditions, wind speed, and the uncertainty in power generation by PV and wind turbine units, the use of batteries as storage systems can lead to an increase in reliability. The amount of energy

stored in the battery at any moment t ($E_{b,t}$) is determined based on Equation (6), wherein P_{charge} and $P_{discharge}$ refer to the charging and discharging power, respectively. Besides, η_{charge} and $\eta_{discharge}$ refer to the charging and discharging efficiency, respectively. η_{auto} is the rate of the battery's self-discharge per hour [41]. Using Equation (6), state of charge (SOC) of the battery energy storage will be as Equation (7), wherein $SOC_{b,t}$ refers to the SOC of battery energy storage at any moment t and $E_{b,total}$ is the total capacity of the battery energy storage in kWh.

$$E_{b,t} = E_{b,(t-1)} \cdot \left(1-\eta_{auto}\right) + P_{charge,t} \cdot \eta_{charge} - \frac{P_{discharge,t}}{\eta_{discharge}} \quad (6)$$

$$SOC_{b,t} = \frac{E_{b,t}}{E_{b,total}} \times 100\% \quad (7)$$

2- 4- Thermal Load Controller

The TLC operates similarly to an electric boiler [42], converting surplus electrical energy into thermal energy to meet heating demands. In this study, the TLC is modeled as a steady-state power-to-heat unit with a fixed thermal conversion efficiency, consistent with the long-term techno-economic scope of the analysis. When renewable generation exceeds the instantaneous electrical load, and the battery bank is fully charged, the surplus power is directed to the TLC to serve the thermal demand. Although detailed dynamic behavior or variable efficiency under partial-load conditions is not explicitly modeled, this representation effectively captures the TLC's role in sector coupling and in enhancing renewable energy utilization. By enabling efficient management of thermal loads, the TLC contributes to a higher renewable fraction, lower fuel consumption, and reduced emissions in the proposed HRES.

3- Proposed Method

3- 1- Economic Equations

Considering that one of the goals of this paper is the economic analysis of using HRESs, it is necessary to determine the use of different resources through an appropriate economic analysis. The net present cost (*NPC*) of a system over *R* years is equal to the present value of the system's costs over its useful life, minus the present value of the system's revenues over its useful life.

The most significant costs of the system include the capital cost (C_{Cap}) and annual operating cost (C_{Op}), including replacement cost (C_{Rep}), maintenance and operation cost ($C_{O\&M}$), emission penalties ($C_{Emission}$), and fuel cost (C_{Fuel}). Sources of revenue for the system include the earnings from energy sold to the grid, which are omitted in this context because of the system's isolated operation, alongside the residual value of equipment linked to its remaining useful life (C_{Sal}). The method of calculating the salvage value of equipment is described in [22].

The system's annual cost (C_{ann}) is calculated according to Equations (8) to (10), where *R* is the useful life of the system, *i* is the real interest rate, *CRF* is the capital recovery factor, i_0 is the nominal interest rate, and *f* refers to the annual inflation rate [43].

$$C_{ann} = CRF\left(i,R\right) \times NPC \quad (8)$$

$$CRF\left(i,R\right) = \frac{i\left(1+i\right)^R}{\left(1+i\right)^R - 1} \quad (9)$$

$$i = \frac{i_0 - f}{1+f} \quad (10)$$

3- 2- Objective Function

The primary objective of this paper is to demonstrate the potential of sector coupling through an off-grid HRES, designed to simultaneously meet electrical and thermal energy demands in rural areas. This method guarantees a sustainable and resilient energy supply by combining RESs with storage options. Therefore, the decision variables of the optimization problem include variables that define the system architecture. Thus, decision variables include the following:

- Capacity of solar panels
- Capacity of wind turbines
- Capacity of battery-based storage resources
- Capacity of inverters
- Capacity of TLCs

The specifications of each equipment and the costs associated with them are inputs to the optimization problem. The goal of minimizing the *NPC* throughout the project's duration serves as the optimization problem's objective function (Equation (11)) [44]:

$$\min \quad NPC = \sum_{n=1}^{N} i\left(C_{Cap,n} + C_{Op,n} - C_{Sal,n}\right) \quad (11)$$

Here, *N* refers to the entire lifecycle of the project, indicated in years.

3- 3- Constraints

The first constraint of the optimization problem is the maximum allowable value of the capacity shortage fraction. A capacity shortage refers to the gap between the needed operational capacity and the actual output capacity that the system can deliver. The annual capacity shortage encompasses the overall shortage observed during the year. The capacity shortage ratio (f_{cs} in %) is calculated by dividing the total capacity shortage (E_{cs} in kWh/year) by the total electrical demand (E_{demand} in kWh/year), as outlined in Equation (12) [45]. It is clear that the lower the maximum allowed value

of f_{cs} is selected in the problem constraints, the higher the reliability of the system will be.

$$f_{cs} = \frac{E_{cs}}{E_{demand}} \tag{12}$$

Another constraint of the optimization problem is the battery's minimum SOC. The majority of rechargeable batteries are not designed for complete discharge, as doing so can lead to irreversible damage in some types of batteries. As such, the minimum state of charge (SOC_{min}) indicates the percentage of total capacity below which the battery storage is not utilized [45]. The constraint for the minimum state of charge of the battery is illustrated in Equation (13).

$$SOC_{b,t} \geq SOC_{\min} \tag{13}$$

The balance of electrical and thermal power at each time is another constraint of the optimization problem. Thus, the generated energy and the consumed energy at each moment of the project's lifetime (except for moments when capacity shortage occurs) must be equal. Regardless of moments when capacity shortage occurs, Equations (14) and (15) can be expressed for the balance constraint of electrical and thermal power, respectively.

$$P_{w,t} + P_{PV,t} + P_{discharge,t}.\eta_{discharge,t} = P_{Electrical\ Load,t} + P_{TLC}^{in} + \frac{P_{charge,t}}{\eta_{charge}} + P_{inv,t}^{loss} \tag{14}$$

$$P_{TLC,t}^{out} + P_{Boiler,t}^{out} = P_{Thermal\ Load,t} \tag{15}$$

Where, $P_{inv,t}^{loss}$ is the power losses in the inverter due to its efficiency less than 100%.

3- 4- Scenarios Description

Considering the modelling approaches applied to various components of the HRES, simulation results are presented in three scenarios in this paper. The first scenario depicts a situation where the entire electrical demand is supplied by the grid, and all thermal demand is met through natural gas combustion in a virtual boiler. The schematic of the first scenario is shown in Fig. 2 (a). In this scenario, the fuel consumption and the emission levels are regarded as the primary concern in traditional networks without the utilization of RESs. In the second scenario, illustrated in Fig. 2 (b), a HRES consisting of PV/wind/battery energy storage is used to meet the electrical energy demand of the system, while natural gas is used to fulfill the system's thermal demand. In the third scenario (Fig. 2 (c)), the integration of a TLC enables sector coupling by utilizing surplus RE to meet thermal demands. This approach demonstrates the potential of sector coupling to enhance the flexibility and sustainability of HRESs. By comparing these scenarios, the impact of employing RESs and TLC to simultaneously meet the electrical and thermal demands on the system costs and pollutant emissions can be observed.

3- 5- Sensitivity Analysis

One of the aspects that is always considered in technical-economic studies is the sensitivity analysis of results in

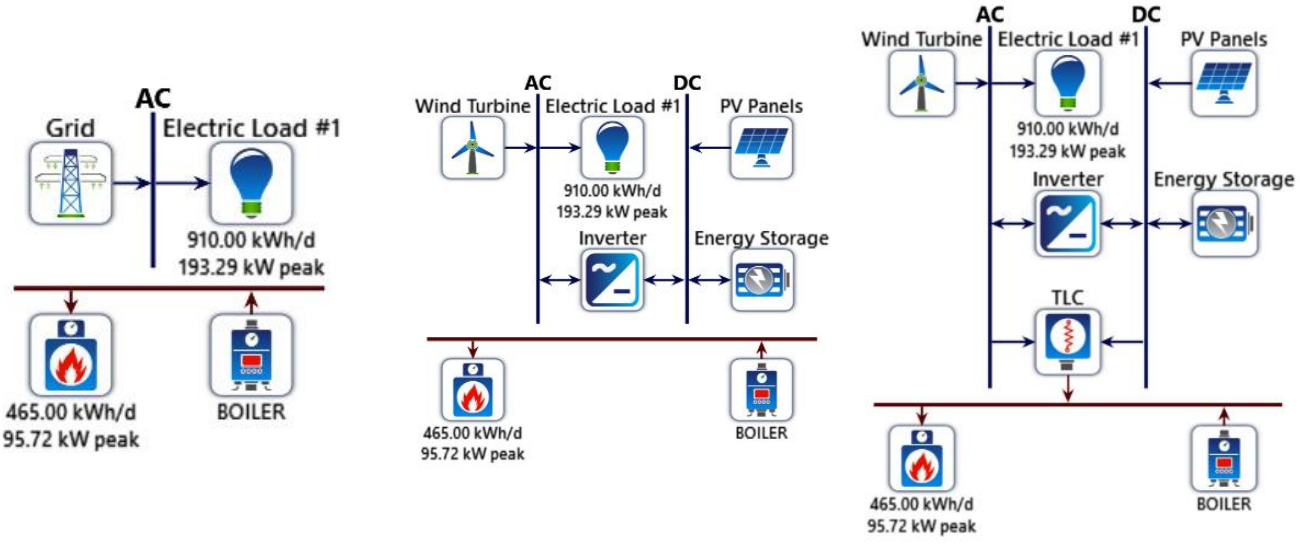

(a) (b) (c)

Fig. 2. The schematic of the electrical-thermal system architecture (a) Scenario #1 (b) Scenario #2 (c) Scenario #3

relation to key variables. To this end, in this paper, several variables are also examined as important variables.

As stated before, one of the existing research gaps in the field of HRESs is the failure to consider the impact of system reliability on the optimal architecture and costs of the system. For this purpose, the capacity shortage fraction is considered as a variable in the problem's constraints. To show the impact of this variable, values of zero, 5%, and 10% are considered as maximum allowable values of capacity shortage fraction in solving the problem.

Due to substantial subsidies on natural gas prices in Iran and the government's announced intention to decrease these subsidies in the near future to discourage improper consumption patterns among certain subscribers, three alternative prices of 0.06 $/m^3$, 0.1 $/m^3$, and 0.5 $/m^3$ are taken into consideration.

In addition, considering the rapid global decline in battery prices due to technological advancements and mass production, the capital cost of the battery is included as another key sensitivity parameter. To represent potential future cost-reduction scenarios, the investment cost of the battery is varied at 90%, 80%, 70%, 60%, and 50% of its current price. This enables assessment of how decreasing storage costs could influence the optimal configuration and economic feasibility of the proposed off-grid system. Further details on this analysis are presented in the subsequent sections.

3- 6- Optimization procedure

The techno-economic optimization of the proposed HRES was performed using the built-in optimizer in HOMER Pro. The software minimizes the total *NPC* by iteratively simulating possible system configurations over an hourly time step. Each configuration is evaluated based on investment, replacement, and operational costs while satisfying power balance and reliability constraints. The optimization variables include the installed capacities of PV panels, wind turbines, battery storage, and the converter, each defined by upper and lower bounds.

HOMER's adaptive optimization routine uses parameters such as the focus factor, system design precision, and *NPC* precision to balance convergence speed and global accuracy. A lower focus factor ensures a broader exploration of the search space, while higher values lead to faster convergence near the current best solution. The process concludes when the changes in both system design and NPC fall below their respective precision thresholds, ensuring a stable and cost-optimal configuration.

4- Implementation

This paper analyzes the proposed power and heat HRES across three scenarios. For simulating and optimizing the suggested HRES, HOMER software was chosen due to its established reliability and common application in renewable energy research. HOMER's systematic modeling approach allows for optimizing renewable energy fractions at the lowest cost, making it a valuable tool for designing resilient and cost-effective hybrid systems. In this study, monthly average wind speed and solar radiation data were utilized due to limited access to high-resolution meteorological records for the selected rural area. HOMER is specifically designed to accept such monthly average inputs and internally converts them into a synthetic hourly time series to perform detailed energy balance and optimization calculations. For instance, for the wind resource, HOMER fits a Weibull probability distribution to the monthly mean wind speeds and generates realistic hourly variations accordingly. This method provides an appropriate balance between data availability and the long-term techno-economic assessment objectives of the present work. Additionally, HOMER's sensitivity analysis capabilities allow for evaluating various system configurations under different economic and technical conditions, providing valuable insights into the robustness and flexibility of the proposed HRES.

The operational control of the proposed system was implemented using HOMER's "microgrid controller" under the "Load Following" strategy. In this approach, renewable generation is first used to supply the instantaneous electrical loads. If additional energy is available, the battery bank is charged until it reaches its maximum SOC, and any remaining surplus can be utilized by the thermal subsystem. When renewable generation decreases and the battery SOC reaches its minimum limit (20%), the unsupplied demand is recorded as unmet electrical load, representing system-level load shedding. HOMER treats the total load as an aggregated profile without differentiating among load priorities, and the unmet load fraction is calculated based on the capacity shortage at each time step.

4- 1- Case Study

The village under study, Qarche village in Tabas county, Yazd province, has a population of 105 people and 28 households. It is located at the geographical coordinates of 34.922500, 57.488889. The monthly temperature curve for Yazd province is depicted in Fig. 3 Considering the warm climate of this region, electricity consumption is higher during the summer months compared to other months of the year. According to the World Bank data, the electricity consumption per capita in Iran is 3160 kWh/year per person [46]. Consequently, it is calculated that the average daily electrical energy usage in this village is roughly 910 kWh. The assumed electrical load curve for Qarche village is shown in Fig. 4. The demand for thermal energy is lower compared to the demand for electrical energy, averaging around 465 kWh/day. The thermal load demand in different months of the year in Qarche is illustrated in Fig. 5. Considering the coordinates of Qarche village, the annual solar irradiation and wind patterns are shown in Fig. 6 and Fig. 7, respectively. These curves are extracted using the HOMER software from NASA's predictions. The daily average solar radiation measures approximately 5.06 kWh/m^2, while the average wind speed is recorded at 5.33 m/s.

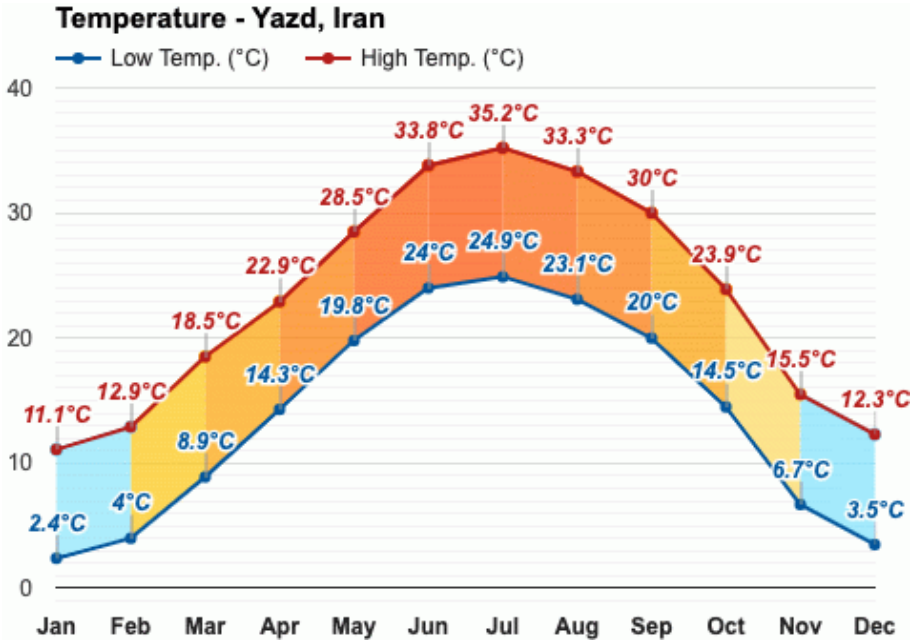

Fig. 3. Monthly temperature variation in Yazd province of Iran [48].

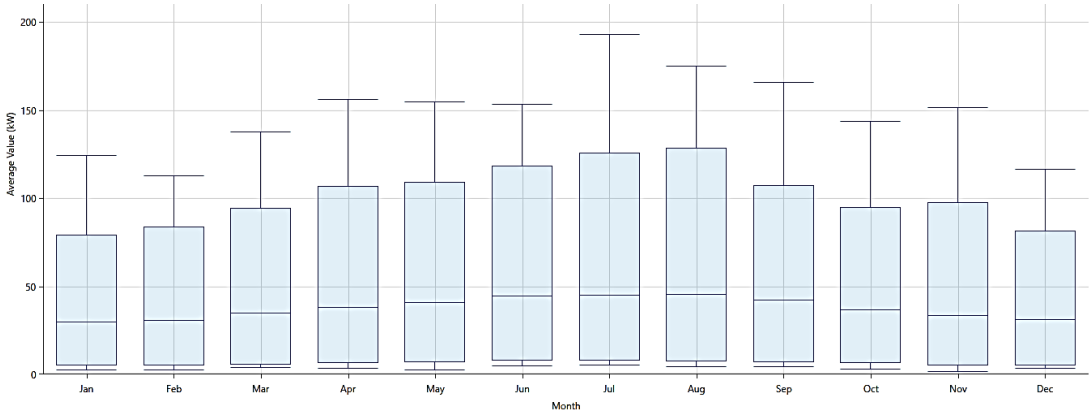

Fig. 4. Electrical power consumption curve for the village of Qarche throughout the year.

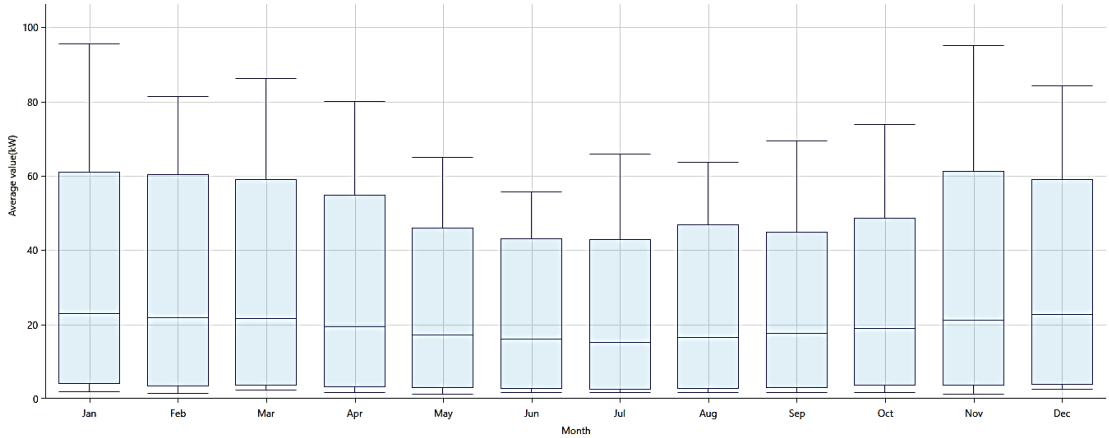

Fig. 5. Thermal power consumption curve for the village of Qarche throughout the year.

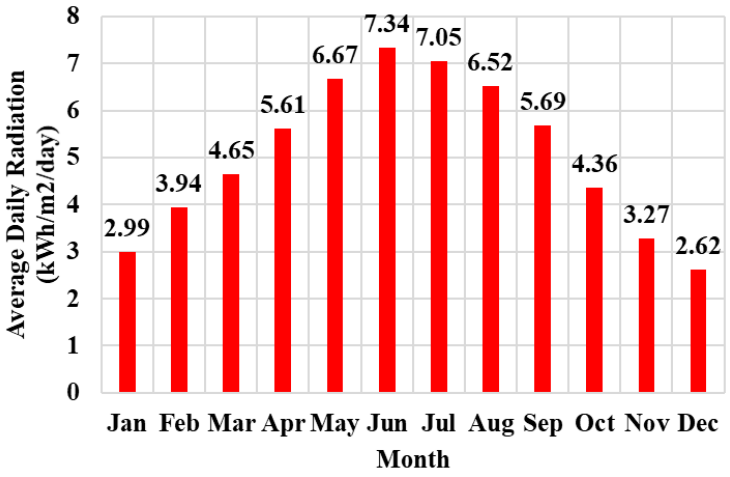

Fig. 6. Monthly variations in average radiation throughout the year in Qarche.

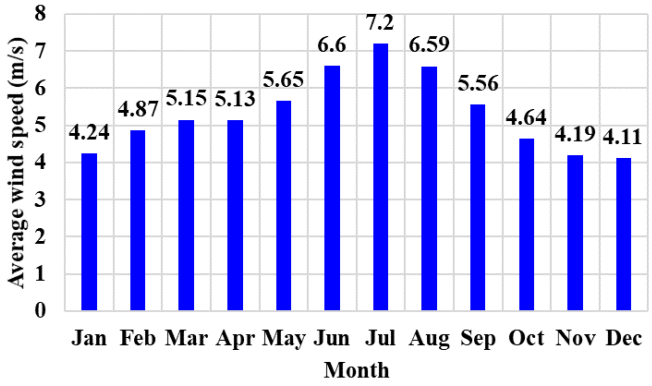

Fig. 7. Average wind speed at a height of 50 meters above ground level in different months of the year in Qarche.

4- 2- Values and Costs

The investment cost and lifespan of solar panels are evaluated at 1200 $/kW and 20 years, respectively [47]. This study utilizes SunPower E20-327 solar panels, which have a nominal output of 327 W, resulting in an investment cost of 392.4 $. Furthermore, the yearly maintenance and repair expenditures amount to 1% of the initial investment [31], totalling 3.924 $/year. Additionally, the coefficients f_{PV} and α_p are considered to be 0.8 and -0.37%/°C, respectively [30].

The cost for investment and replacement of the inverter is estimated at 300 $/kW, excluding any maintenance expenses [30]. The lifespan of the inverters is assumed to be 20 years, with a 95% efficiency rating [30]. Utilizing 10 kW inverters in this research implies an investment equivalent to 3000 $.

Table 3 outlines the specifications and costs associated with the wind turbine utilized in this study.

In this paper, a battery with a capacity of 72 kWh and 30 kW, a lifespan of 20 years, and investment and maintenance costs of respectively, $4400 and $8 is considered [50]. The charging and discharging efficiency is 95%, and the battery's self-discharge rate is also considered to be 0.02% [41]. Considering that fully discharging batteries can reduce their lifespan, the minimum allowable state of charge for the batteries is set to 20%.

The capital cost of the TLC is estimated to be 54 $/kW with a lifespan of 20 years [51].

Finally, the system's useful life, annual inflation rate, and the interest rate are considered to be 20 years, 30% [10], and 18% [22], respectively.

4- 3- Fuel Specifications and Emission Penalties

Using diesel fuel in the boiler of a HRES results in the emission of pollutants such as carbon dioxide, carbon monoxide, unburned hydrocarbons, particulate matter, sulfur dioxide, and nitrogen oxides. Emission penalties are incurred for releasing pollutants into the atmosphere, providing incentives to justify the use of HRES. These penalties vary from state to state. The national energy balance report for Iran

Table 3. Details regarding the 10 kW wind turbine utilized in this research [45, 49].

Specification	Value
Capacity (kW)	10
Rotor diameter (m)	15.81
Hub height (m)	36
Cut-in wind speed (m/s)	2.75
Cut-out wind speed (m/s)	20
Investment cost ($)	24000
Maintenance cost ($/year)	240
Lifespan (year)	20

Table 4. The average levels of primary pollutant emissions in Iran and the related penalties for exceeding those limits [22].

Emission particle	Emissions content (g/kWh)	Emissions Penalties ($/ton)
Carbon Dioxide	660.650	2.86
Carbon Monoxide	0.620	54
Unburned Hydrocarbons	18.018	60
Particulate Matter	0.120	1228.60
Sulfur Dioxide	1.660	521.50
Nitrogen Oxides	2.380	171.50

Table 5. The specifications of natural gas for meeting the thermal loads in Iran.

Properties	Value
Lower Heating Value (MJ/kg)	45
Density (kg/m^3)	0.790
Carbon Content (%)	67
Sulfur Content (%)	0

(2015) contains information on emission levels and penalties related to major pollutants, as demonstrated in Table 4. To ensure that penalties are applied and to encourage the use of REs, the upper limit for all emissions was set at zero due to the very low emissions of the system.

Given the abundant natural gas resources in Iran, the fuel used for domestic heating in Iran is natural gas. Natural gas is readily available throughout Iran via the gas distribution system, covering urban and rural areas. Utilizing REs to meet the heating load in rural areas can play an effective role in reducing gas distribution network costs and decreasing pollutant emissions.

The specifications of natural gas for meeting the heating load are presented in Table 5. Additionally, a system efficiency of 85% is considered for the heating supply system.

4- 4- Scenarios Results

4- 4- 1- Scenario #1

In this scenario, the assumed cost for purchasing electricity from the grid is 0.012 $/kWh. In this scenario, the entire energy demand of the system is supplied by fossil fuels. The annual consumption of fuel is 20,220 m^3, which is used to meet the thermal load. The annual electrical energy consumption is 332,150 kWh, which is supplied by the grid.

Table 6. Annual emissions for various pollutants in scenario #1.

Pollutant	Quantity	Unit
Carbon Dioxide	249,645	kg/yr
Carbon Monoxide	330	kg/yr
Unburned Hydrocarbons	9,585	kg/yr
Particulate Matter	63.8	kg/yr
Sulfur Dioxide	551	kg/yr
Nitrogen Oxides	1,266	kg/yr

Table 7. Annualized costs of the system in scenario #1.

Name	Capital	Operating	Salvage	Resource	Total
Boiler	$0.0	$0.0	$0.0	$1213	$1213
Grid	$0.0	$3,986	$0.0	$0.0	$3986
Other	$0.0	$1,890	$0.0	$0.0	$1890
System	$0.0	$5,876	$0.0	$1213	$7089

Table 8. The sensitivity of the total annual system costs for different values of natural gas fuel prices in scenario #1.

Natural Gas Fuel Price ($/m^3)	Total Annual System Costs ($)
0.06	7,089
0.1	7,898
0.5	15.986

The annual emissions for meeting the electrical and thermal loads of the system are shown in Table 6. A summary of the annual system costs is presented in Table 7. In this table, the price of natural gas purchase is considered to be 0.06 $/m^3. The penalty costs for emissions are accounted for under the "Others" category of expenses. Moreover, the total annual system costs for different values of natural gas fuel prices are presented in Table 8. As no alternative solution is suggested for meeting the thermal load, an increase in the natural gas fuel price leads to higher annual system costs.

4- 4- 2- Scenario #2

In this scenario, the electrical load is supplied by the proposed HRES based on PV/Wind/Battery Energy Storage instead of the grid. However, similar to the previous scenario, the thermal load is met by burning natural gas in a virtual boiler. The optimal results for the system architecture considering the sensitivity to the different values of capacity shortage values are presented in Table 9. Since there is only one choice available to meet the thermal load in this scenario by a virtual boiler, changes in natural gas prices do not affect the optimal system architecture. Therefore, variations in natural gas prices are not considered in this table.

Considering that the solar energy potential is higher than wind energy in Qarche, the main challenge lies in supplying electrical demand during nighttime hours. Therefore, there is a need for a large amount of battery energy storage to meet the electrical demand during nighttime hours. To substantiate this claim, the SOC of the battery energy storage throughout the year for the first row of Table 9 (Capacity Shortage = 0) is illustrated in Fig. 8. As observed, the batteries are fully charged during the daylight hours when solar panels reach their maximum output, and they discharge during nighttime hours. It is worth noting that, to prolong battery lifespan, a minimum SOC of 20% is considered in the problem constraints. By increasing the allowable capacity shortage, a 10 kW wind turbine is added to the optimal system architecture to increase electricity generation during nighttime hours. In contrast, the capacity of solar panels and the quantity of storage batteries is reduced to achieve the lowest possible *NPC*.

Table 9. The optimal architecture of the system in scenario #2 for different values of capacity shortage.

Capacity Shortage (%)	PV Panels (kW)	Wind Turbines (kW)	Number of Battery Energy Storages	*NPC* ($)	Total Fuel (m³/year)	PV Panels Production (kWh/year)	Wind Turbines Production (kWh/year)	Energy Storage Annual Throughput (kWh/year)	Renewable Fraction (%)
0	151.31	40	17	700,444.70	20,220.40	242,599.20	315,768.30	83,959.98	66.18
5	96.36	50	10	569,225.60	20,220.40	154,499.20	394,710.30	65,524.27	65.71
10	80.44	50	7	522,487.70	20,220.40	128,971.50	394,710.30	58,506.36	65.16

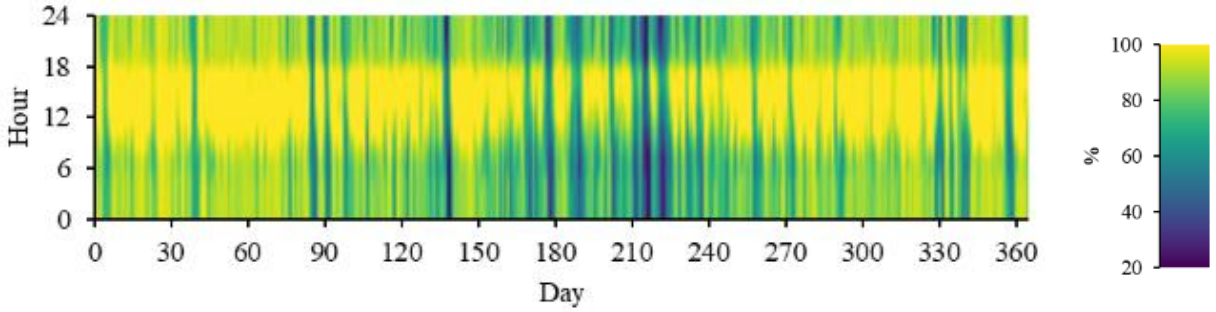

Fig. 8. The battery energy storage SOC during the year in scenario #2

The sensitivity of *NPC* and energy storage annual throughput variations to the maximum allowed value of f_{cs} is depicted in Fig. 9. As observed, with an increase in the maximum allowed value of f_{cs} from 0% to 5% and 10%, the *NPC* value has decreased from $770,444.70 to $569,225.60 and 522,487.70, equivalent to a 26.1% and 32.2% reduction in system costs, respectively. Besides, the energy storage annual throughput is decreased from 83959.98 kWh/year to 65524.27 kWh/year and 58506.36 kWh/year, equivalent to a 22.0% and 30.3% reduction in energy storage annual throughput, respectively. Thus, with a slight decrease in system reliability, almost more than one-fourth of the system costs and one-fifth of the energy storage annual throughput is reduced. Therefore, in cases where the electrical load of the system is of low importance, a trade-off can be made between *NPC* and system reliability to reduce system costs. Furthermore, in cases where battery energy storage maintenance and repair hold greater importance, this trade-off can occur between energy storage annual throughput and system reliability. It is worth mentioning that each system variable can be involved in the trade-off and is not limited to these two variables.

The renewable fraction represents the share of energy provided to the load originating from RESs. As shown in Table 9, the maximum allowed value of f_{cs} has a negligible effect on the share of REs in providing the total energy required by the system. In this scenario, the entire electrical load of the system is supplied by RESs, while the entire thermal load of the system is met by fossil fuels. Overall, approximately 66% of the energy required is supplied by RESs. In contrast, in the previous scenario, the share of RESs in the supply system energy was zero.

Considering that the entire thermal load is provided by a virtual boiler, the emissions level in all cases in Table 9 remains the same. The emissions level in this scenario is shown in Table 10. Since the renewable fraction is increased, there is a significant reduction in pollutant emissions compared to scenario #1 (Table 6).

4- 4- 3- Scenario #3

In this scenario, TLC is utilized to increase the share of REs in the overall energy demand of the system. As mentioned, TLC can convert excess electrical energy into thermal energy. In other words, the possibility of meeting the thermal load using REs is achieved through the utilization of TLC in this scenario.

The sensitivity of the optimal system architecture to different values of f_{cs} and natural gas fuel price values are presented in Table 11. As indicated in Table 11, with the addition of TLC and the possibility of meeting the thermal load using RESs, the renewable fraction has increased compared to scenario #2. Considering that the solar energy potential in

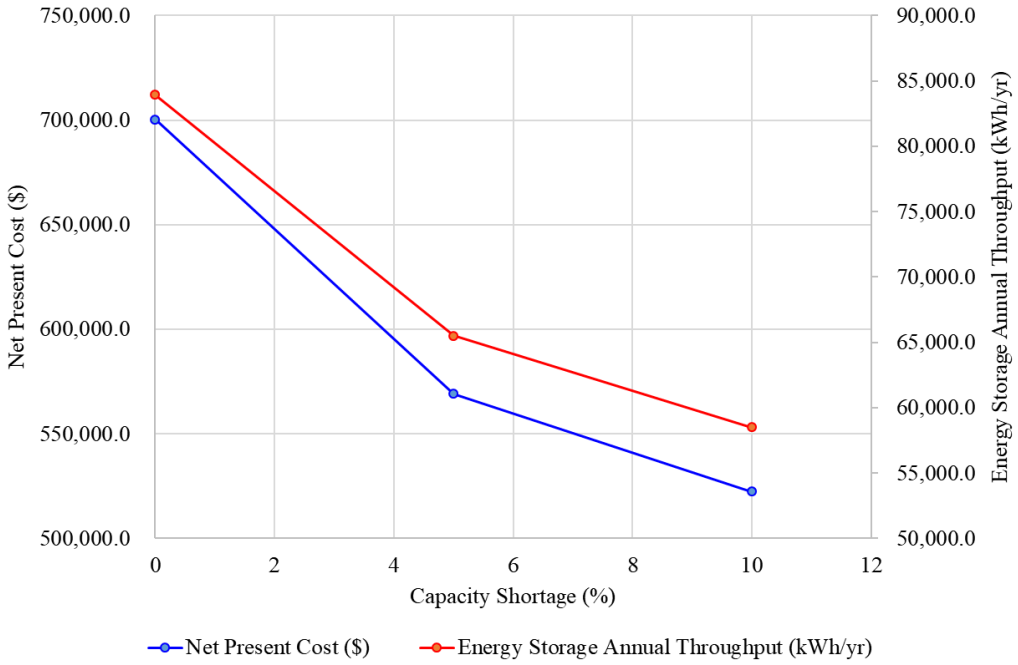

Fig. 9. The variations of NPC and energy storage annual throughput based on maximum annual capacity shortage in scenario #2

Table 10. Annual emissions for various pollutants in scenario #2

Pollutant	Quantity	Unit
Carbon Dioxide	30,210	kg/yr
Carbon Monoxide	124	kg/yr
Unburned Hydrocarbons	3,598	kg/yr
Particulate Matter	24.0	kg/yr
Sulfur Dioxide	0	kg/yr
Nitrogen Oxides	475	kg/yr

Qarche is greater than wind energy, the challenge of meeting the system's energy demand during nighttime hours is more difficult than meeting it during daytime hours. Therefore, the number of wind turbines has increased with the rise in natural gas prices to reduce the need for using batteries and natural gas to supply electrical and thermal loads during nighttime, respectively. Furthermore, with the increase in natural gas prices, the capacity of TLC in the optimal system architecture has increased to provide a greater renewable fraction and reduce fuel consumption.

Another point that stands out in Table 11 is the reduction in *NPC* in similar conditions compared to scenario #2. For better comparison, a comparison between *NPC* in scenarios #2 and #3 is shown in Table 12. As observed, the use of TLC not only has increased the renewable fraction in the system but also contributed to a decrease in the overall *NPC*. The decrease in *NPC* is attributed to the reduction in costs associated with natural gas fuel and the penalty for pollutant emissions. A comparison of pollutant emission levels for the first row of Table 9 (scenario #2) and Table 11 (scenario #3) is presented in Fig. 10. As illustrated in this figure, the emission levels, and consequently, the penalty resulting from pollutant emissions in scenario #3 is significantly decreased due to the implementation of TLC for meeting thermal loads using RESs.

Another point illustrated in Table 12 is the sensitivity of the *NPC* to the system reliability (maximum allowed value of f_{cs}). Therefore, considering the importance of electrical load, a compromise can be made between *NPC* and the desired reliability of the system. For a better understanding of this matter, the sensitivity of *NPC* relative to changes in capacity shortage at various values of natural gas fuel price are depicted in Fig. 11.

Table 13 represents a comparison of the contribution of each energy source in meeting the electrical and thermal loads for the first and last rows of Table 11. As observed,

Table 11. The optimal architecture of the system in scenario #3 for different values of capacity shortage and natural gas fuel price.

Capacity Shortage (%)	Natural Gas Fuel Price ($/m³)	PV Panels (kW)	Wind Turbines (kW)	Number of Energy Storage	TLC (kW)	*NPC* ($)	Total Fuel (m³/year)	PV Production (kWh/year)	Wind Turbine Production (kWh/year)	Energy Storage Annual Throughput (kWh/year)	Renewable Fraction (%)
0	0.06	130.74	50	15	155.0	625511.1	10533.45	209620.00	394710.3	70071.57	82.37
5	0.06	70.06	50	10	96.8	515148.7	11750.37	112333.20	394710.3	58311.71	79.67
10	0.06	46.75	50	7	74.5	412328.9	12109.50	74952.77	394710.3	44410.07	78.30
0	0.1	131.28	50	15	155.0	651041.4	10523.17	210474.80	394710.3	70028.88	82.39
5	0.1	65.93	60	7	108.0	491178.1	9446.13	105708.30	473652.3	48100.52	83.65
10	0.1	45.55	50	10	73.6	454271.1	12170.82	73029.35	394710.3	44828.76	78.19
0	0.5	137.58	70	11	184.0	883511.8	7153.36	220584.40	552594.4	51207.01	88.03
5	0.5	54.92	80	6	121.0	701364.9	6924.55	88044.34	631536.5	37300.31	88.01
10	0.5	30.17	80	3	102.0	634262.7	7009.93	48363.95	631536.5	24434.87	87.44

Table 12. Comparison between scenario #2 and #3 under the same conditions in terms of capacity shortage and natural gas fuel price.

Capacity Shortage (%)	0	5	10	0	5	10	0	5	10
Natural Gas Fuel Price ($/m³)	0.06	0.06	0.06	0.1	0.1	0.1	0.5	0.5	0.5
NPC Scenario #2	700,444.7	569,225.6	522,487.7	752,473.5	621,254.4	574,721.4	1,272,761.0	1,141,542.0	1,102,099.0
NPC Scenario #3	625,511.1	515,148.7	412,328.9	651,041.4	491,178.1	454,271.1	883,511.8	701,364.9	634,262.7

Table 13. Annual emissions for various pollutants in scenario #2.

Capacity Shortage (%)	Natural Gas Fuel Price ($/m³)	Electric Source	kWh/year	%	Thermal Source	kWh/year	%
0	0.06	PV Panels	209,620	34.7	Generic Boiler	88,415	26.5
		Wind Turbines	394,710	65.3	TLC	244,906	73.5
		Total	604,330	100	Total	333,321	100
10	0.5	PV Panels	48,364	7.11	Generic Boiler	58,840	13.7
		Wind Turbines	631,536	92.9	TLC	371,828	86.3
		Total	679,900	100	Total	430,667	100

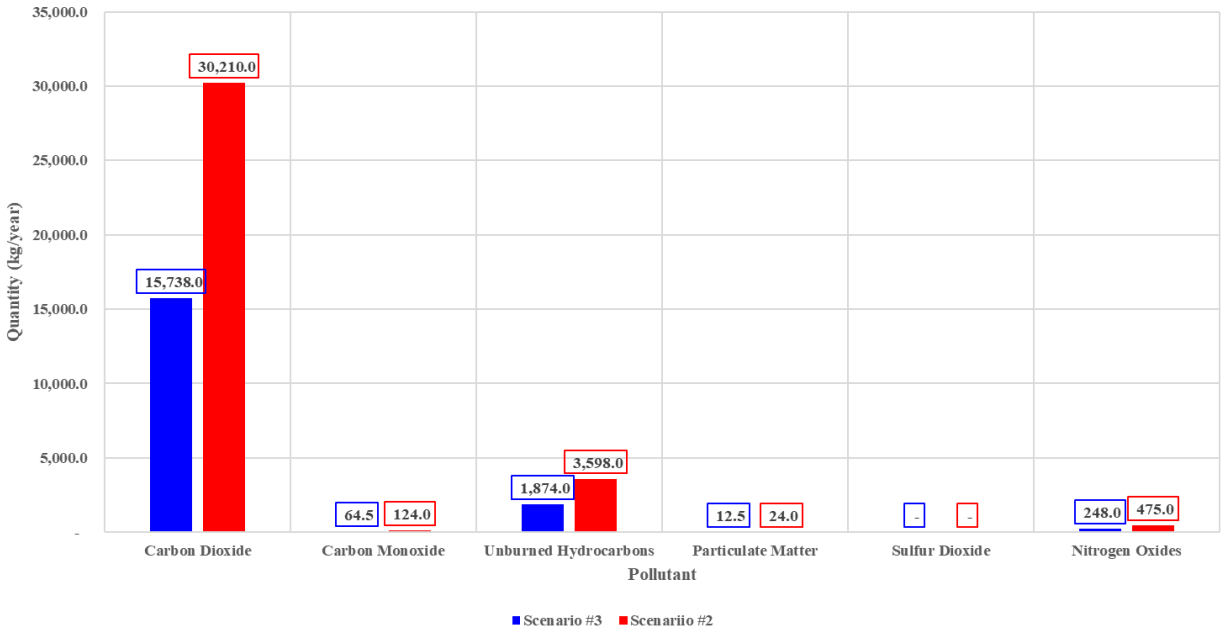

Fig. 10. The comparison of pollutant emission levels for the first row of Table 9 (scenario #2) and Table 11 (scenario #3).

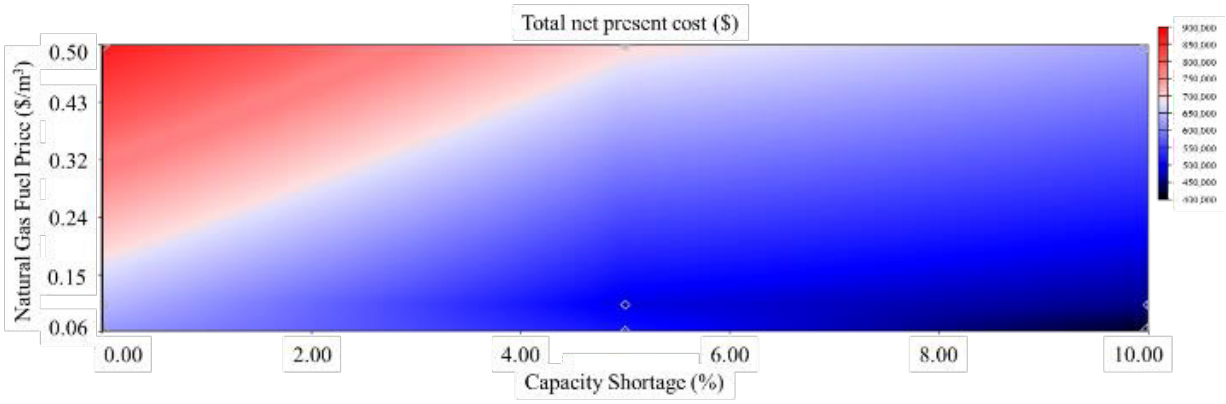

Fig. 11. Surface plot of NPC considering the system reliability and natural gas fuel price variations in scenario #3.

despite the greater potential of solar energy in the Qarche, for achieving minimum *NPC*, a greater use of wind turbines to meet the energy demand during nighttime hours is more reasonable compared to using battery energy storage. Thus, the share of wind turbine generation relative to solar panels in the total electricity produced throughout the year is higher. For thermal load, a significant portion is allocated to TLC, while the remaining thermal load is supplied using natural gas. With an increase in natural gas fuel price, the share of TLC in meeting the thermal load has also increased. In these conditions, to increase the share of TLC, especially during night-time hours, the optimum system configuration includes a greater number of wind turbines to lessen fuel consumption and minimize *NPC*. Consequently, in these conditions, the share of wind turbine generation has also increased relative to solar panels.

Table 14 illustrates the sensitivity of the optimal system configuration to variations in the investment cost of batteries, ranging from 100% to 50% of the current cost. As observed, the reduction in battery price significantly affects the optimal system architecture and techno-economic indicators. With decreasing battery costs, the optimal number of battery units gradually increases, enabling greater utilization of renewable resources. Consequently, the total fuel consumption and *NPC* exhibit a clear downward trend as the energy storage capacity becomes more affordable.

In parallel, the installed capacity of PV panels increases as battery prices decline, while the capacity of wind turbines

Table 14. Effect of battery cost reduction on optimal system configuration and techno-economic indicators.

Battery cost (% of base)	PV (kW)	Wind (kW)	Number of Energy Storage	*NPC* ($)	PV production (kWh/yr)	Wind production (kWh/yr)	Fuel (m^3/yr)	Renewable fraction (%)	Battery throughput (kWh/yr)
100% (base)	30.17	80	3	634,263	48,365	631,537	7,009.9	87.4	24,435
90%	35.0	78	4	602,550	56,108	615,748	6,659.4	88.5	32,580
80%	40.0	75	5	570,836	64,123	592,065	6,308.9	89.5	40,725
70%	45.0	72	6	539,123	72,139	568,383	5,958.4	90.5	48,870
60%	50.0	70	7	520,095	80,154	552,594	5,607.9	91.5	57,015
50%	60.0	65	8	494,725	96,185	513,123	4,906.9	93.0	65,160

Table 15. Comparative summary of relevant studies.

Reference	Case Study	Location	Grid Connection	Considered Sectors	Load Detail	Renewable Fraction (%)	CO2 Reduction (%)
[10]	Oil Refinery	Iran	On-grid	Electrical	1800 MWh/day	Max. 68.8	44.6
[22]	Village	Iran	On-grid	Electrical	431 kWh/day	Max. 68.3	Not Reported
[31]	Agricultural wells	Iran	Off-grid	Electrical	Between 30-220 kW	100	100
[29]	Village	Bangladesh	Off-grid	Electrical	Essential load: 1108 kWh/day Deferrable load: 75kWh/day	Max. 100	100
This Study	Village	Iran	Off-grid	Electrical & Thermal	Electrical: 910 kWh/day Thermal: 465 kWh/day	Max. 88.03	93.69

shows a moderate reduction. This behavior can be attributed to the improved capability of storing excess solar energy during daytime hours for use at night, which decreases the system's reliance on wind energy to meet nighttime demand. The enhanced energy storage capability also leads to higher annual battery throughput, demonstrating a more dynamic charge–discharge cycle that supports renewable integration and grid stability.

Overall, the renewable energy fraction rises steadily from approximately 87% at the current battery cost to over 93% when the battery cost is reduced by half. This improvement highlights the critical role of energy storage in increasing renewable penetration and reducing fossil fuel dependency in off-grid hybrid systems. The observed reduction in *NPC* further confirms that advancements in battery technology and cost reduction can considerably improve the economic feasibility and sustainability of rural off-grid HRESs.

4- 4- 4- Comparison with Previous Studies

To further demonstrate the significance and novelty of the proposed HRES, Table 15 compares the main features and performance indicators of this study with several representative works reported in the literature. The selected studies differ in location, system scale, grid connection type, and sectoral applications, providing a diverse context for comparison.

Key parameters such as the type of load considered, renewable energy fraction, and CO2 emission reduction are included to enable a consistent evaluation of techno-environmental performance. As shown below, the proposed off-grid HRES designed for combined electrical and thermal demands in a rural context of Iran demonstrates considerable advantages in both renewable fraction and emission reduction compared with previous studies.

The comparative results presented in Table 15 clearly highlight the originality and improved performance of the

Table 16. Techno-economic performance of the natural gas generator-based system under various sensitivity conditions.

Gen100 Heat Recovery Ratio (%)	Natural Gas Fuel Price ($/m³)	*NPC* ($)	Operating cost ($/yr)	Renewable Fraction (%)	Total Fuel (m³/yr)	Gen100 Production (kWh)	Gen100 Fuel (m³/yr)	BOILER Fuel Consumption (m³/yr)	CO2 Emission (kg/year)
0	0.06	1881171	28727.73	0	88112.63	327224.8	67892.22	20220.4	131648.8
100	0.06	1776153	27095.18	0	67899.02	327224.8	67892.22	6.806647	101447.7
0	0.1	2107892	32252.24	0	88112.63	327224.8	67892.22	20220.4	131648.8
100	0.1	1950863	29811.14	0	67899.02	327224.8	67892.22	6.806647	101447.7
0	0.5	4375102	67497.29	0	88112.63	327224.8	67892.22	20220.4	131648.8
100	0.5	3697960	56970.75	0	67899.02	327224.8	67892.22	6.806647	101447.7

present work. Unlike the majority of previous studies that focused solely on electrical loads, the proposed system integrates both electrical and thermal energy sectors, enabling a more comprehensive utilization of renewable resources.

While the renewable fraction achieved in this study (88.03%) is slightly lower than that of fully renewable off-grid systems reported in [29] and [31], this difference is primarily due to the dual-sector design and inclusion of thermal loads, which inherently increase the system's total energy demand. Nevertheless, the proposed configuration attains a remarkably higher CO2 reduction (93.69%), indicating superior overall efficiency and environmental performance.

Compared with the on-grid systems analyzed in [10] and [22], the present off-grid model demonstrates greater energy independence and self-sufficiency, reflecting its potential applicability in remote or isolated regions. These results confirm that the integration of a TLC and an optimized dispatch strategy significantly enhances both the economic and environmental sustainability of hybrid systems in real-world rural applications.

4- 4- 5- Comparative fossil-fuel benchmark: Natural gas generator-based supply

To assess the techno-economic and environmental performance of a conventional fossil-fuel–based system, an additional comparative analysis was conducted in which the electrical load of the village was supplied solely by a 100 kW natural gas generator. The thermal demand was met using the same boiler unit modeled in the previous scenarios. The capital cost and annual operation and maintenance (O&M) cost of the generator are set to 33,200 $ and 0.285 $/operating hour {Toghyani, 2024 #1132}, respectively, with a lifetime of 15,000 hours {Kasaeian, 2019 #916}. The generator fuel type is natural gas, and its efficiency and heat recovery characteristics are modeled according to the HOMER guidelines.

To capture both conventional and cogeneration (CHP[1]) configurations, two levels of the heat recovery ratio were evaluated:

- 0%, representing a simple power generation mode;
- 100%, representing a CHP mode where waste heat is fully utilized for thermal loads.

Therefore, the impacts of fuel price and heat recovery ratio are analyzed as sensitivity parameters. The results of this assessment are summarized in Table 16, which presents the variations of *NPC*, annual operating cost, RE fraction, total fuel consumption, CO2 emission, and generator and boiler performance metrics under different sensitivity conditions.

As shown in Table 16, even under the most favorable configuration, when the generator operates as a CHP unit with full heat recovery, the overall *NPC* remains significantly higher than that of the renewable-based scenarios (Scenarios 2 and 3). In all cases, the RE fraction equals zero, and both annual fuel consumption and operating cost are markedly higher compared to HRESs.

To evaluate the environmental implications, the annual CO2 emissions associated with each sensitivity case are calculated. The results clearly indicate that the natural gas–based configuration produces substantially higher emissions than the HRESs. Even with heat recovery fully enabled, the total CO2 emissions remain well above those of Scenarios 2 and 3.

These findings highlight that, although cogeneration can marginally improve the overall efficiency of a fossil-fuel–based system, its techno-economic and environmental performance still falls short of HRESs. Therefore, integrating renewable resources not only minimizes operational costs and emissions but also enhances long-term sustainability for rural energy systems.

1. Combed Heat and Power

5- Conclusion

This paper introduces an off-grid HRES aimed at integrating the electrical and thermal sectors in rural areas, providing a sustainable approach to energy accessibility. In the design of the system architecture, various factors such as available energy potentials, relationships governing energy sources, system reliability, equipment costs, pollutant emissions, penalty costs of emissions, and fuel costs are considered. The results clearly demonstrate that under different conditions, and with respect to the constraints of the problem, various combinations of RESs can be utilized to minimize the *NPC*. Additionally, sensitivity analysis on the *NPC* relative to the system's reliability demonstrates that, given the significance of meeting the system's energy requirements, it is feasible to compromise on significantly reducing the system's costs at the expense of lowering the system's reliability. Moreover, the sensitivity analysis on battery investment costs revealed that reductions in battery prices strongly influence the optimal configuration and techno-economic performance of the proposed HRES.

A comparative evaluation using a 100 kW natural gas generator—with and without heat recovery—further confirmed that even in the CHP configuration with maximum heat recovery, the *NPC* and emissions remain higher than those of the renewable-based HRES.

A significant increase in the share of renewable energy sources in simultaneously meeting the electrical and thermal loads of the system, along with sustainable development by reducing pollutant emissions, is another important outcome achieved through the utilization of off-grid HRESs in this study.

References

[1] S. Mandelli, J. Barbieri, R. Mereu, E. Colombo, Off-grid systems for rural electrification in developing countries: Definitions, classification and a comprehensive literature review, Renewable and Sustainable Energy Reviews, 58 (2016) 1621-1646.

[2] F.C. Robert, S. Gopalan, Low cost, highly reliable rural electrification through a combination of grid extension and local renewable energy generation, Sustainable cities and society, 42 (2018) 344-354.

[3] K. Nyarko, T. Urmee, J. Whale, Y. Simsek, Y. Haigh, Assessing the effectiveness of energy policies in accelerating renewable energy-based mini-grid deployment: A case study, Energy for Sustainable Development, 85 (2025) 101631.

[4] P. Pandiyan, R. Sitharthan, S. Saravanan, N. Prabaharan, M.R. Tiwari, T. Chinnadurai, T. Yuvaraj, K. Devabalaji, A comprehensive review of the prospects for rural electrification using stand-alone and hybrid energy technologies, Sustainable energy technologies and assessments, 52 (2022) 102155.

[5] A.S. Irshad, W.K. Samadi, A.M. Fazli, A.G. Noori, A.S. Amin, M.N. Zakir, I.A. Bakhtyal, B.A. Karimi, G.A. Ludin, T. Senjyu, Resilience and reliable integration of PV-wind and hydropower based 100% hybrid renewable energy system without any energy storage system for inaccessible area electrification, Energy, 282 (2023) 128823.

[6] T. Falope, L. Lao, D. Hanak, D. Huo, Hybrid energy system integration and management for solar energy: A review, Energy Conversion and Management: X, (2024) 100527.

[7] H. Shahbakhsh, M. Osanloo, Greenhouse Gas Emissions Reduction through Integration of Renewable and Non-renewable Energy Sources: A Model for Sangan Iron Ore Mine Complex of Iran, International Journal of Engineering, 38(11) (2025) 2547-2563.

[8] F. Amiri, M. Eskandari, M.H. Moradi, Improved load frequency control in power systems hosting wind turbines by an augmented fractional order PID controller optimized by the powerful owl search algorithm, Algorithms, 16(12) (2023) 539.

[9] A.K. Bansal, Sizing and forecasting techniques in photovoltaic-wind based hybrid renewable energy system: A review, Journal of Cleaner Production, 369 (2022) 133376.

[10] M. Toghyani, A. Saadat, From challenge to opportunity: Enhancing oil refinery plants with sustainable hybrid renewable energy integration, Energy Conversion and Management, 305 (2024) 118254.

[11] A. Shalbafian, F. Amiri, S. Ganjefar, Adaptive Robust Nonlinear Optimal Sliding Mode Control for Wind Turbines: A Hybrid OHAM-Based Approach to Maximize Power Capture, IET Renewable Power Generation, 19(1) (2025) e70131.

[12] D. Gielen, F. Boshell, D. Saygin, M.D. Bazilian, N. Wagner, R. Gorini, The role of renewable energy in the global energy transformation, Energy strategy reviews, 24 (2019) 38-50.

[13] E. Mohammadian Amiri, S. Ebrahimi, Presenting a Model for Multiple-Step-Ahead-Forecasting of Volatility and Conditional Value at Risk in Fossil Energy Markets, AUT Journal of Modeling and Simulation, 50(1) (2018) 83-94.

[14] S. Backe, M. Korpås, A. Tomasgard, Heat and electric vehicle flexibility in the European power system: A case study of Norwegian energy communities, International Journal of Electrical Power & Energy Systems, 125 (2021) 106479.

[15] R. Rezaei, M. Ghofranfarid, Rural households' renewable energy usage intention in Iran: Extending the unified theory of acceptance and use of technology, Renewable energy, 122 (2018) 382-391.

[16] IRENA, Renewable capacity statistics 2025, 2025.

[17] Global Solar Atlas, in.

[18] M.F.H. Mojumder, T. Islam, P. Chowdhury, M. Hasan, N.A. Takia, O. Farrok, Techno-economic and environmental analysis of hybrid energy systems for

remote areas: A sustainable case study in Bangladesh, Energy Conversion and Management: X, 23 (2024) 100664.

[19] P. Roy, J. He, T. Zhao, Y.V. Singh, Recent advances of wind-solar hybrid renewable energy systems for power generation: A review, IEEE Open Journal of the Industrial Electronics Society, 3 (2022) 81-104.

[20] L. Meng, M. Li, H. Yang, Enhancing energy efficiency in distributed systems with hybrid energy storage, Energy, 305 (2024) 132197.

[21] P. Tarassodi, J. Adabi, M. Rezanejad, Energy Management of an Integrated PV/Battery/Electric Vehicles Energy System Interfaced by a Multi-port Converter, International Journal of Engineering, 36(8) (2023) 1520-1531.

[22] A. Kasaeian, P. Rahdan, M.A.V. Rad, W.-M. Yan, Optimal design and technical analysis of a grid-connected hybrid photovoltaic/diesel/biogas under different economic conditions: A case study, Energy Conversion and Management, 198 (2019) 111810.

[23] X. Xu, Z. Zhang, J. Yuan, J. Shao, Design and multi-objective comprehensive evaluation analysis of PV-WT-BG-Battery hybrid renewable energy systems in urban communities, Energy Conversion and Management: X, 18 (2023) 100357.

[24] H. Chanda, E. Mohareb, M. Peters, C. Harty, Environmental and social impacts of self-financed solar PV adoption in rural Zambia: Insights from mopane worms, mushrooms, fishing, bushmeat and ethnomedicine, Energy for Sustainable Development, 85 (2025) 101665.

[25] M. Ranjbar Jaferi, S. Mohammadi, M. Mohammadian, A Novel Intelligent Energy Management Strategy Based on Combination of Multi Methods for a Hybrid Electric Vehicle, AUT Journal of Modeling and Simulation, 46(2) (2014) 31-46.

[26] M. Hosseinzadeh, F. Rajaei Salmasi, Supervisory control of a hybrid AC/DC micro-grid with load shedding based on the bankruptcy problem, AUT Journal of Modeling and Simulation, 48(1) (2016) 3-12.

[27] T. Sarkar, A. Bhattacharjee, H. Samanta, K. Bhattacharya, H. Saha, Optimal design and implementation of solar PV-wind-biogas-VRFB storage integrated smart hybrid microgrid for ensuring zero loss of power supply probability, Energy conversion and management, 191 (2019) 102-118.

[28] A.S. Irshad, N. Kargar, M. Elkholy, G.A. Ludin, S. Elias, A. Hilali, T. Senjyu, M.M. Gamil, G. Pinter, Techno-economic evaluation and comparison of the optimal PV/Wind and grid hybrid system with horizontal and vertical axis wind turbines, Energy Conversion and Management: X, (2024) 100638.

[29] M.S. Islam, R. Akhter, M.A. Rahman, A thorough investigation on hybrid application of biomass gasifier and PV resources to meet energy needs for a northern rural off-grid region of Bangladesh: A potential solution to replicate in rural off-grid areas or not?, Energy, 145 (2018) 338-355.

[30] M. Bagheri, N. Shirzadi, E. Bazdar, C.A. Kennedy, Optimal planning of hybrid renewable energy infrastructure for urban sustainability: Green Vancouver, Renewable and sustainable energy reviews, 95 (2018) 254-264.

[31] A. Heydari, A. Askarzadeh, Optimization of a biomass-based photovoltaic power plant for an off-grid application subject to loss of power supply probability concept, Applied Energy, 165 (2016) 601-611.

[32] K. Murugaperumal, S. Srinivasn, G.S. Prasad, Optimum design of hybrid renewable energy system through load forecasting and different operating strategies for rural electrification, Sustainable Energy Technologies and Assessments, 37 (2020) 100613.

[33] R.F. Ferreira, R.A.M. Lameirinhas, C.P.C.V. Bernardo, J.P.N. Torres, M. Santos, Agri-PV in Portugal: How to combine agriculture and photovoltaic production, Energy for Sustainable Development, 79 (2024) 101408.

[34] R. Song, T. Hamacher, V. Terzija, V.S. Perić, Potentials of using electric-thermal sector coupling for frequency control: A review, International Journal of Electrical Power & Energy Systems, 151 (2023) 109194.

[35] M.R. Ghodsi, F. Barati, Performance Assessment of a Laboratory Rooftop PV Plant in Karaj-Iran, International Journal of Engineering, 38(9) (2025) 2104-2113.

[36] A. Khosravani, E. Safaei, M. Reynolds, K.E. Kelly, K.M. Powell, Challenges of reaching high renewable fractions in hybrid renewable energy systems, Energy Reports, 9 (2023) 1000-1017.

[37] M. Karamsima, F. Jahangiri, M. Nourimanzar, Fuzzy Model Reference Adaptive Pitch Control of a Variable Speed Wind Turbine in the Full-load Region, AUT Journal of Modeling and Simulation, 56(2) (2024) 209-218.

[38] V. Fazlollahi, M. Taghizadeh, F. Ayatollah Zade Shirazi, Modeling and neuro-fuzzy controller design of a wind turbine in full-load region based on operational data, AUT Journal of Modeling and Simulation, 51(2) (2019) 139-152.

[39] M. Toghyani, A. Abedi, M. Barahoei, Solar and Wind-Based Hybrid Technologies, in: Reference Module in Earth Systems and Environmental Sciences, Elsevier, 2023.

[40] P. Gipe, Wind energy comes of age, John Wiley & Sons, 1995.

[41] J. Vergara-Zambrano, W. Kracht, F.A. Díaz-Alvarado, Integration of renewable energy into the copper mining industry: A multi-objective approach, Journal of Cleaner Production, 372 (2022) 133419.

[42] J. Yu, L. Guo, M. Ma, S. Kamel, W. Li, X. Song, Risk assessment of integrated electrical, natural gas and district

heating systems considering solar thermal CHP plants and electric boilers, International Journal of Electrical Power & Energy Systems, 103 (2018) 277-287.

[43] A. Kumar, A. Biswas, Techno-economic Optimization of a Stand-alone Photovoltaic-battery Renewable Energy System for Low Load Factor Situation- a Comparison between Optimization Algorithms, International Journal of Engineering, 30(10) (2017) 1555-1564.

[44] X. Li, J. Gao, S. You, Y. Zheng, Y. Zhang, Q. Du, M. Xie, Y. Qin, Optimal design and techno-economic analysis of renewable-based multi-carrier energy systems for industries: A case study of a food factory in China, Energy, 244 (2022) 123174.

[45] H. Pro, Homer Pro 3.14 user manual, Boulder, CO, USA, (2017).

[46] Energy consumption in Iran, in.

[47] S. Bhattacharjee, A. Dey, Techno-economic performance evaluation of grid-integrated PV-biomass hybrid power generation for rice mill, Sustainable Energy Technologies and Assessments, 7 (2014) 6-16.

[48] Weather Atlas, in.

[49] S. Bhattacharjee, R. Das, G. Deb, B.N. Thakur, Techno-economic analysis of a grid-connected hybrid system in Portugal Island, Int J Comput Sci Eng, 7 (2019) 1-14.

[50] Y. Basheer, A. Waqar, S.M. Qaisar, T. Ahmed, N. Ullah, S. Alotaibi, Analyzing the Prospect of Hybrid Energy in the Cement Industry of Pakistan, Using HOMER Pro, Sustainability, 14(19) (2022) 12440.

[51] O. Aalde, Hybrid renewable-diesel energy systems in an off-grid arctic community of Svalbard, Norwegian University of Life Sciences, 2018.

HOW TO CITE THIS ARTICLE

E. Sadeghi, M. Gholami, Electric–Thermal Sector Coupling with Hybrid Renewables and Storage for Sustainable Rural Energy Systems, AUT J. Elec. Eng., 58(1) (2026) 167-188.

DOI: 10.22060/eej.2025.24451.5707